THE ASTROPHYSICAL JOURNAL, 301:727–741, 1986 February 15

AN ANALYSIS OF THE NARROW LINE PROFILES IN SEYFERT 2 GALAXIES[1]

M. M. DE ROBERTIS AND D. E. OSTERBROCK
Lick Observatory, Board of Studies in Astronomy and Astrophysics, and University of California, Santa Cruz
Received 1985 May 8; accepted 1985 August 14

ABSTRACT

An analysis of the line profiles in 18 high-ionization Seyfert 2 galaxies is presented. Two-thirds of the sample show a correlation between emission-line width and critical density. Few objects show a correlation between line width and ionization potential. [O III] λ4363 appears broader than [O III] λ5007 in 70% of the galaxies, whereas [O I] λ6300 is broader than [S II] λ6716 in 66% of the cases. This argues strongly for a model in which optically thick emission-line clouds occupy regions of highest density and velocity dispersion. In some galaxies, however, optically thin clouds contribute significantly to emission in the low-ionization lines.

The fraction of the featureless continuum at 5000 Å is estimated using the equivalent widths of the Mg I λ5176 and Fe I λ5270 absorption features. A correlation was found between the Hβ emission-line equivalent width and the line widths for all emission lines. According to the relation, all narrow-line widths tend to 320 ± 25 km s^{-1} as the Hβ emission-line equivalent width approaches zero. This value may correspond to the minimum velocity produced by the acceleration mechanism or, for flattened emission-line regions, to the velocity dispersion perpendicular to the plane. No other significant correlations are found between emission-line widths and other measured parameters.

The nonparametric Wilcoxon rank-sum test is used to test the hypothesis that the Seyfert 2 line profile widths presented here and the corresponding Seyfert 1 narrow-line profile widths presented in De Robertis and Osterbrock are taken from the same underlying distribution. When the small systematic velocity difference between the techniques used to measure the Seyfert 1 and the Seyfert 2 galaxies of this paper is taken into account, the mean FWHM for the low-ionization lines is found to be larger in the Seyfert 2 galaxies. Lines of high ionization *and* critical density, [O III] λ4363 and [Fe VII] λ6087, are on average significantly broader in Seyfert 1 Galaxies. Some of the physical implications of these results are discussed.

The Seyfert 2 line widths are compared with a small sample of narrow emission-line galaxies observed and reduced in the same manner. Each galaxy is briefly discussed. [Fe X] λ6375 and [Fe VII] λ6087 are found to vary substantially on time scales of a few years in I Zw 92.

Subject headings: galaxies: Seyfert — line profiles

I. INTRODUCTION

The similarities and differences between Seyfert 1 and Seyfert 2 galaxies present an outstanding problem in active galactic research. One way of approaching this problem is to study the nuclear emission-line profiles in both types of galaxies. De Robertis and Osterbrock (1984; hereafter Paper I) presented an analysis of the narrow emission-line profiles in a sample of high-ionization Seyfert 1 and 1.5 galaxies (and one Seyfert 2). The present work, an investigation of the line profiles in Seyfert 2 galaxies, is intended as a complementary study.

To be classified as a Seyfert 2, a galaxy's nuclear emission-line spectrum must show a wide range of ionization, with an [O III] λ5007/Hβ intensity ratio of at least 3 (Shuder and Osterbrock 1981; Baldwin, Phillips, and Terlevich 1981). Lines representing low stages of ionization such as [O I] and [S II] must be present as well, indicating indirectly the presence of a nonstellar photoionizing continuum. By definition, Seyfert 2 spectra do not have broader permitted lines (which characterize Seyfert 1s), but instead have permitted line widths similar to forbidden line widths. The emission lines must have a full width at half-maximum (FWHM) ≥ 300 km s^{-1} (Shuder and Osterbrock 1981). (There is also a morphological restriction which separates Seyfert galaxies from QSOs: Seyfert galaxies must have a bright, semistellar nucleus and show the definite presence of an underlying galaxy.) All the Seyfert galaxies in this sample satisfy these criteria.

For a review of the conditions in the emission-line regions refer to Paper I. In brief, it appears that the narrow emission lines in Seyfert 2 galaxies, as with Seyfert 1s, originate in gas clouds with electron densities $\sim 10^{3-6}$ cm^{-3} at distances $\sim 10^{1}$–10^{3} pc from the central continuum source. There is evidence of very weak broad-line emission in the Seyfert galaxy NGC 1068 from polarization studies (Miller and Antonucci 1983), and hence of the presence of broad-line material. It is by no means a typical Seyfert 2, but there are indications of similar weak broad-line emission in Mrk 3 (Miller, private communication). The suggestion that all Seyfert 2s may have weak broad-line emission is not an unreasonable extrapolation.

It is not clear what differences exist, if any, between the photoionizing continuum sources in Seyfert 2s and 1s, because it has not been possible to observe the photoionizing continuum for a substantial number of Seyfert 2s (or even a large sample of Seyfert 1s). There is evidence that the mean absolute optical luminosities of the continuum sources are greater for Seyfert 1s than 2s, but this conclusion may be affected by a number of selection effects (Koski 1978). Essentially the same power law fits the featureless continuum slope between the optical spectral region and the X-ray region (near 2 keV) in Seyfert 1 and 2 galaxies (Ferland and Osterbrock 1985).

[1] *Lick Observatory Bulletin*, No. 1021.

Although there is very little X-ray spectral information for Seyfert 2s, they are on average intrinsically less X-ray luminous than Seyfert 1s (Elvis and Lawrence 1985). Also it is not clear if the tendency for broad-line objects (including Seyfert 1s) to exhibit "big" and "little" UV "bumps" (e.g., see Ferland and Shields 1985), while narrow-line objects (like Seyfert 2s) do not, implies that there are important differences in the continuum sources within the broad and narrow-line objects, respectively.

Finally, it is not clear to what extent differences in the radio characteristics of the two populations might be related to the narrow emission-line profiles. Ulvestad and Wilson (1984) have confirmed that Seyfert 2s statistically appear more luminous in the radio region. They also suggested that the nonthermal pressures inferred from the radio observations in Seyfert 2s might provide the mechanism that confines the narrow-line clouds and filaments. Under this interpretation, it would not be surprising to find a statistical difference between Seyfert 1 and 2 narrow emission-line profiles.

II. SAMPLE AND MEASUREMENTS

This sample of Seyfert 2 galaxies was chosen from among the highest ionization Seyfert 2s observed by Osterbrock and collaborators within the past several years. All the spectra were obtained with the image-dissector scanner (IDS) (Robinson and Wampler 1972; Miller, Robinson, and Wampler 1976; Miller, Robinson, and Schmidt 1980) on the Shane 3 m telescope of Lick Observatory. They were taken with a 1200 line mm^{-1} grating, giving a wavelength coverage of 1280 Å and an instrumental resolution of 5 Å. Many of the Seyfert galaxies in this sample were observed during the past year at this high resolution, their high-ionization emission-line spectra (containing He II λ4686, [Fe VII] λ6087, or even [Fe X] λ6375) having been noted from previous lower resolution Lick scans. Finally, the Seyfert galaxies were selected to be bright enough so that data of sufficiently high signal-to-noise ratios could be obtained in reasonable exposure times.

Table 1 presents a summary of the relevant information for the galaxies contained in this sample. The names of each galaxy are listed in column (1); the Seyfert "type" designation in column (2); the heliocentric redshifts (obtained by taking the average redshift of Hβ and [O III] $\lambda\lambda$4959, 5007) are in column (3). The equivalent widths of the Hβ and [O III] λ5007 relative to the observed continuum are presented in columns (4) and (5), respectively. Columns (6) and (7) list the measured equivalent widths of the Mg I *b* λ5176 and Fe I E2 λ5270 absorption features. Column (8) gives the fraction of featureless continuum at 5000 Å for each galaxy, assuming that the Mg I *b* and Fe I E2 equivalent widths relative to the stellar continuum are those of a "normal" galaxy. (We will discuss this in more detail below.) An estimate of the monochromatic continuum luminosity at 5000 Å is provided in column (9). These estimates may be uncertain by $\sim$10%–20% since a slit of 2".7 × 4".0 was used for the observations of both the standard stars and the Seyfert nuclei.

On average, typical Seyfert 2 galaxies have lower ionization than typical Seyfert 1 galaxies (Cohen 1983). However, there are enough high-ionization Seyfert 2s represented that this difference should not prove to be a serious impediment to the investigation. Since the photoionizing continua have similar forms (Ferland and Osterbrock 1985), the difference must be due to some combination of the typically lower luminosity of the featureless continuum in typical Seyfert 2s, and of a possible greater mean distance of the emission-line region from the central source.

For comparison with the Seyfert 2 galaxies, we also obtained similar data for a few galaxies that have emission lines in their spectra, but are not Seyfert galaxies. All of them appear to be galaxies in which nuclear gas is photoionized by OB stars. One, NGC 7177, is a normal barred spiral with very weak emission lines; the others are all objects with fairly strong emission lines, similar to those of H II regions, that we call simply "narrow emission-line galaxies." The "comparison galaxy" parameters are listed in Table 2 according to name and redshift. The emission-line identifications and FWHMs given in this table will be discussed below. One galaxy, M81, has a very weak broad Hα emission component (Peimbert and

TABLE 1

SEYFERT GALAXIES OBSERVED

Galaxy (1)	Type (2)	z (3)	W(Hβ) (Å) (4)	W(λ5007) (Å) (5)	W(Mg I *b*) (Å) (6)	W(E2) (Å) (7)	f_{FC} (8)	log (L_{5000})[a] (ergs s^{-1} $Å^{-1}$) (9)
NGC 2110	2[b]	0.0077	20	92	2.7	0.5	0.50	38.33
NGC 5506	2[b]	0.0065	64	555	2.9	...	0.40	37.80
NGC 7212	2	0.0265	64	756	4.3	0.4	0.80	38.96
NGC 7319	2	0.0209	19	157	4.5	...	0.10:	38.70
Mrk 1	2	0.0160	63	667	2.4	...	0.45	38.46
Mrk 3	2	0.0132	64	865	4.1	...	0.25:	38.81
Mrk 78	2	0.0363	89	230	1.3	0.0	0.75:	39.32
Mrk 348	2	0.0148	21	300	2.2	0.4	0.70	38.76
Mrk 516	1.8	0.0282	5	14	1.7	1.5	0.33	39.23
Mrk 573	2	0.0170	26	337	5.2	...	0.25:	38.93
Mrk 1018	1.9	0.0417	1	21	3.9	3.2	0.10:	39.84
Mrk 1058	2	0.0172	4	50	3.2	1.4	0.30	38.85
Mrk 1066	2	0.0118	25	89	3.0	0.7	0.50	38.72
Mrk 1073	2	0.0230	33	223	1.0	0.8	0.75	39.00
Mrk 1157	2	0.0151	16	187	3.2	1.0	0.40	38.66
I Zw 92	2	0.0375	91	1010	2.4	1.1	0.50	39.65
UM 16	2	0.0585	24	369	0.0	0.0	0.95	39.44
Akn 347	2	0.0220	7	96	3.8	...	0.60	39.30

[a] Monochromatic (5000 Å) continuum luminosity; $q_0 = 0$, $H_0 = 75$ km s^{-1} Mpc^{-1}.

[b] X-ray selected galaxy (see text).

TABLE 2

NARROW EMISSION-LINE GALAXIES

Galaxy	z	Wavelength (Å)	FWHM (km s^{-1})	Quality
NGC 6951	0.0042	5007	200	2
NGC 7177	0.0037	3727	310[a]	1
		6563	290	2
		6583	380	2
		6716	350	1
Mrk 309	0.0430	4340	360	2
		4861	300	2
		5007	430	1
Akn 160	0.0230	4861	160	2
		5007	0[b]	1
		6300	190	2
		6563	130	2
		6583	170	2
		6716	220	2
Haro 25	0.0254	4363	0[b]	2
		4861	60	1
		4959	90	1
		5007	70	1
M81	0.0163	5007	280	1
		6300	300	2
		6563	270	2
		6583	270	2
		6731	260	2

[a] Deblended as described in text.
[b] Narrower than instrumental profile.

Torres-Peimbert 1981; Shuder and Osterbrock 1981) and might be classified as a "Seyfert 1.95" galaxy; another, Mrk 309, shows strong Wolf-Rayet or Of star features in the integrated spectrum of its nucleus, and obviously has a large population of highly evolved luminous O stars (Osterbrock and Cohen 1982).

Since Seyfert 2 galaxies do not have broad lines, profile analysis is somewhat easier for them than for Seyfert 1s. However, since the mean optical fluxes of these Seyfert 2 nuclei are appreciably fainter than for the Seyfert 1s, the signal-to-noise ratio is, on average, somewhat smaller. It is well known there is often a substantial stellar contribution to the observed continuum in Seyfert 2s in addition to the underlying power law (Koski 1978). The Seyfert 2 spectra in this sample, except those indicated in § IV, do not appear to be dominated by an underlying stellar continuum. Since this is the case, and since we are primarily concerned with the narrow line widths, we have not attempted more complicated, and sometimes subjective, stellar continuum removal techniques, but rather used the "best-fit continuum" determined by eye.

A complete list of the lines measured in at least some of the galaxies is presented in Table 3. In order, the columns contain the stage of ionization, the wavelength of the transition, the ionization potential of the lower stage of ionization (to produce the relevant ion), the ionization potential of the upper stage (to remove the ion), and the critical density at 10^4 K of the term that emits the line.

In the emission-line analysis, blends were treated as in Paper I; when necessary, the $\lambda\lambda$4340, 4363 pair was deblended assuming that the Hγ profile could be represented by the Hβ profile (from the same scan) multiplied by an appropriate scale factor. [S II] $\lambda\lambda$6716, 6731 were deblended using the initial assumption that the profiles were approximately identical. After two or three interactions from this initial condition, very good approximations to the deblended profiles were produced using RETICENT (Pritchet, Mochnacki, and Yang 1982). It was found empirically that the FWHMs measured for these profiles are not overly sensitive to this assumption. In cases where the atmospheric B absorption band clearly affected one of the lines, its FWHM was not listed in Table 4. In other cases

TABLE 3

IONIZATION POTENTIALS AND CRITICAL DENSITIES

Stage of Ionization	Wavelength (Å)	Ionization Potential Lower (eV)	Ionization Potential Upper (eV)	Critical Density (cm^{-3})
[Ne V]	3426	97.1	126.2	1.6E7
[O II]	3727	13.6	35.1	4.5E3
[Ne III]	3869	41.0	63.5	9.7E6
He I	3889	24.6	54.4	...
[Ne III]	3967	41.0	63.5	9.7E6
[S II]	4069	10.4	23.3	2.6E6
Hδ	4101	13.6	...	...
Hγ	4340	13.6	...	...
[O III]	4363	35.1	54.9	3.3E7
He II	4686	54.4	...	...
Hβ	4861	13.6	...	...
[O III]	4959	35.1	54.9	7.0E5
[O III]	5007	35.1	54.9	7.0E5
[N I]	5199	0.0	14.5	2.0E3
[Fe VII]	5721	99.1	125.	3.6E7
He I	5876	24.6	54.4	...
[Fe VII]	6087	99.1	125.	3.6E7
[O I]	6300	0.0	13.6	1.8E6
[Fe X]	6375	233.6	262.1	4.8E9
[N II]	6548	14.5	29.6	8.7E4
Hα	6563	13.6	...	...
[N II]	6583	14.5	29.6	8.7E4
[S II]	6716	10.4	23.3	1.5E3
[S II]	6731	10.4	23.3	3.9E3

TABLE 4

SEYFERT GALAXY LINE-PROFILE WIDTHS

Galaxy (1)	Wavelength (Å) (2)	FWHM (km s^{-1}) (3)	Quality (4)
NGC 2110	3727	650	1
	3869	510	1
	4069	530	2
	4340	630	2
	4363	530	3
	4861	690	1
	4959	590	1
	5007	570	1
	5199	510	2
	6300	600	1
	6563	570	1
	6583	530	1
	6716	440	1
	6731	440	1
NGC 5506	4340	510	1
	4363	330	2
	4686	400	2
	4861	390	1
	4959	370	1
	5007	370	1
	5199	390	2
	6300	340	1
	6563	390	1
	6583	300	1
	6716	370	1
	6731	370	1
NGC 7212	3727	520	1
	3869	400	1
	3889	380	1
	3967	490	2
	4069	830	3
	4101	410	1
	4340	430	1
	4363	510	2
	4686	450	2
	4861	440	1
	4959	420	1
	5007	410	1
	5199	460	2
	5876	460	2
	6087	730	3
	6300	520	1
	6563	510	1
	6583	590	1
	6716	490	1
	6731	470	1
NGC 7319	4340	500	2
	4363	490	3
	4686	310	3
	4861	480	1
	4959	370	1
	5007	390	1
	6300	400	1
	6563	470	1
	6583	470	1
	6716	490	1
Mrk 1	3727	660	1
	3869	550	1
	3889	620	2
	3967	600	1
	4069	820	2
	4101	630	2
	4340	630	1
	4363	800	2
	4686	480	2
	4861	650	1
	4959	670	1
	5007	610	1
	5199	720	3
	5876	580	1
	6087	920	3
	6300	670	1
	6563	660	1
	6583	560	1
	6716	450	1
	6731	490	1
Mrk 3	4363	880	3
	4686	880	3
	4861	870	1
	4959	860	1
	5007	840	1
	5199	570	2
	5876	930	3
	6300	760	1
	6563	710	1
	6583	710	1
	6716	660	1
Mrk 78	3727	920	1
	3869	720	2
	4861	710	1
	4959	690	1
	5007	680	1
	5876	660	2
	6300	880	1
	6563	570	1
	6583	710	1
	6731	600	1
Mrk 348	4340	470	2
	4363	360	3
	4686	250	3
	4861	380	1
	4959	350	1
	5007	370	1
	5199	410	3
	6300	290	1
	6563	320	1
	6583	300	1
	6716	260	1
Mrk 516	4861	280	3
	5007	460	3
	6300	310	3
	6563	350	1
	6583	380	1
	6716	340	2
Mrk 573	3727	500	1
	3869	290	1
	3889	370	2
	3967	280	1
	4069	420	2
	4101	300	1
	4340	310	1
	4363	320	2
	4686	320	2
	4861	300	1
	4959	290	1
	5007	300	1
	5199	230	3
	5876	460	2
	6087	380	1

TABLE 4—*Continued*

Galaxy (1)	Wavelength (Å) (2)	FWHM (km s^{-1}) (3)	Quality (4)
	6300	290	1
	6375	400	3
	6563	370	1
	6583	400	1
	6716	310	1
	6731	290	1
Mrk 1018	4861	520	3
	4959	380	1
	5007	370	1
	6716	430	3
	6731	360	3
Mrk 1058	4861	200	3
	4959	280	1
	5007	250	1
	6300	300	3
	6563	260	2
	6583	250	2
	6716	280	2
Mrk 1066	4861	350	1
	4959	450	1
	5007	440	1
	5199	380	2
	6300	420	1
	6563	400	1
	6583	350	1
	6716	330	1
	6731	330	1
Mrk 1073	3727	560	1
	3869	360	1
	3889	470	2
	3967	410	2
	4069	440	3
	4101	240	2
	4340	380	1
	4686	340	2
	4861	360	1
	4959	340	1
	5007	360	1
	5876	500	2
	6087	280	3
	6300	360	1
	6563	370	1
	6583	330	1
	6716	320	1
Mrk 1157	4340	260	1
	4363	510	2
	4686	320	2
	4861	260	1
	4959	310	1
	5007	300	1
	5199	310	2
	5876	260	2
	6300	320	1
	6563	270	1
	6583	290	1
	6716	270	1
I Zw 92	3426	650	2
	3727	510	1
	3869	460	1
	3889	590	2
	3967	530	2
	4069	530	2
	4101	360	3
	4340	280	2
	4363	500	1
	4686	520	2
	4861	330	1
	4959	350	1
	5007	380	1
	5199	210	2
	5876	390	2
	6087	490	2
	6300	300	1
	6375	530	3
	6563	360	1
	6583	260	1
	6716	270	1
	6731	280	1
UM 16	3727	500	1
	3869	300	1
	3967	450	2
	4069	870	3
	4101	310	2
	4340	330	1
	4363	310	2
	4686	300	1
	4861	300	1
	4959	350	1
	5007	420	1
	5721	360	2
	5876	440	2
	6087	640	2
	6300	280	1
	6563	380	2
	6583	340	1
	6716	270	1
	6731	330	1
Akn 347	4363	480	3
	4686	220	2
	4861	310	1
	4959	410	1
	5007	320	1
	6087	260	3
	6300	380	2
	6563	330	2
	6583	330	2
	6716	400	2
	6731	370	2
	6300	200	3
	6563	330	2
	6583	340	2
	6731	260	3

where one component was much "cleaner" than the other, only the better has been presented. The [S II] λλ4069, 4076 blend was treated in the same way. [Fe X] λ6375, when present, was isolated by using the profile of [O I] λ6300 to remove [O I] λ6364. The Hα [N II] λλ6548, 6583 blend was more difficult to separate. An iterative technique like that for [S II] was used, but the resulting measurements are not as reliable as for unblended profiles.

At a resolution of 5 Å, [O II] λ3727 appears as a single profile, although it is a blend of λλ3726.0, 3728.8. We used the results of an empirical test to estimate the "true" FWHM of an unblended [O II] profile. The [O III] λ5007 profile from an "average" Seyfert 2 galaxy was used to model both [O II] λ3726.0 and λ3728.8 (appropriately transformed in velocity space), and to synthesize [O II] λ3727. For a sequence of intensity ratios, the measured FWHM of this blend was compared with the "true" FWHM of the initial unblended profiles. Over a wide range of intensity ratios, it was found that the ratio of the measured to "true" FWHM was 1.35 to better than a few percent. Considering that the [O III] profiles are probably not identical to the [O II] profiles and that this empirical factor will almost certainly vary somewhat from object to object, to a first approximation it is not unreasonable to use it to obtain a deblended FWHM for [O II] λ3727. In Table 4 the FWHM for [O II] λ3727 is given as measured (i.e., blended), whereas in Figures 1 and 2 the profile was deblended using this empirical factor.

The FWHM for each of the unblended profiles was then obtained by marking the continuum beneath the profile, generating a second order-least-squares fit to the central five channels to locate the maximum, and interpolating in wavelength to find the two points on the profile at the half-maximum level. To determine the relevant instrumental profile we followed the technique used by Osterbrock and Pogge (1985). The FWHMs of all unblended lines from the comparison lamps were measured, and a second-order least-squares fit was carried out between wavelength and instrumental FWHM. This fit accounts approximately for the slight difference in focus between the center and edges of the field. The full amplitude of the instrumental FWHM differences in a single scan is ~10%. The intrinsic FWHM of each line profile was then calculated as the square root of the difference between the squares of the FWHMs of the observed line profile and of the interpolated "instrumental" profile. We have not applied deconvolution techniques to these data chiefly because our main interest is in obtaining "characteristic" widths for the lines and not in a quantitative analysis of the entire profiles. With line widths close to the instrumental widths, and signal-to-noise ratios slightly less than those of Paper I, deconvolution techniques become more difficult.

The results of these measurements are quoted in Table 4. For each galaxy, the rest wavelength of each line is listed in column (1), and the rest FWHM is given in (2) to the nearest 10 km s^{-1}. Column (3) gives a rough estimate of the "line quality," with "1" being excellent, "2" good, and "3" poor–fair (usually the result of difficulties in continuum placement or severe blending). The (internally consistent) errors in the FWHM measures are ~10% for lines of quality 1, and 20% or more for lines of quality 3. As with the profiles in Paper I, the ambiguity in the continuum placement generally contributes to the largest FWHM uncertainty. Similar information is listed in Table 2 for the narrow emission-line galaxies.

III. INDIVIDUAL OBJECTS

The following provides a brief description of the important or unique details of the individual Seyfert 2 galaxies of the present sample.

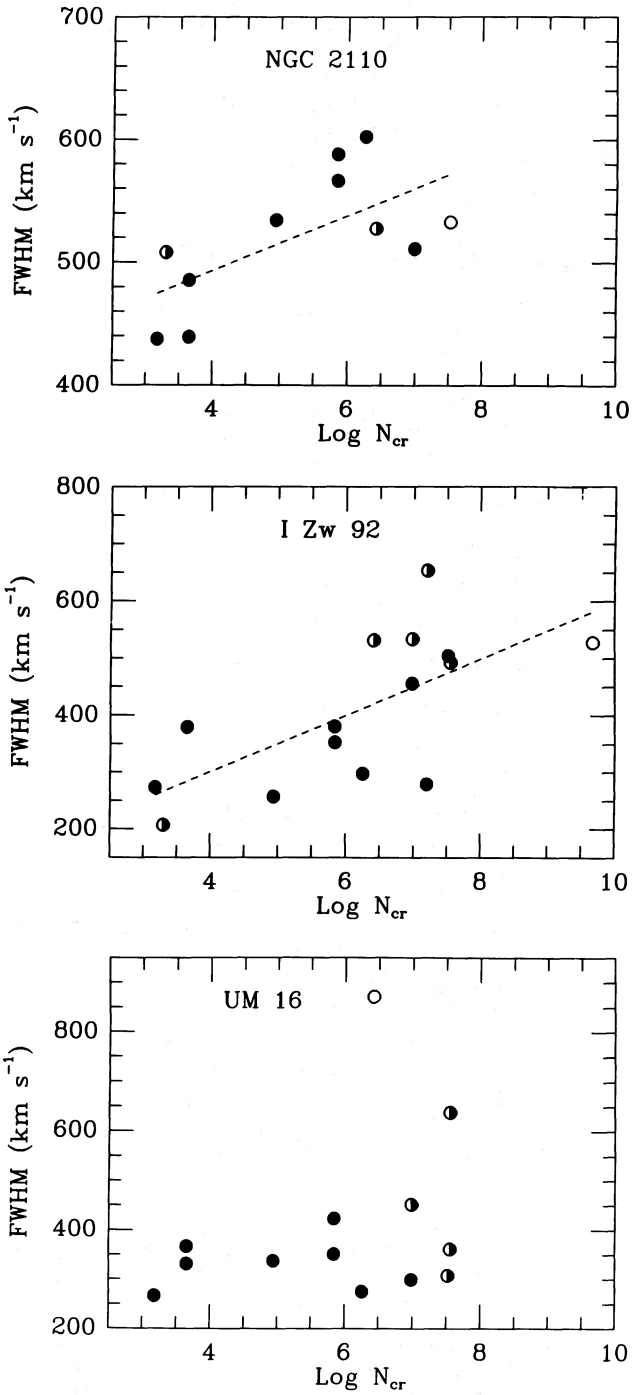

FIG. 1.—Correlations of emission-line widths at half-maximum (FWHM) with logarithm of the critical density for (*a*) NGC 2110, (*b*) I Zw 92, and (*c*) UM 16. Filled circles denote quality 1 profiles (see text), half-filled circles denote quality 2 profiles, and open circles denote quality 3 profiles. Dashed lines in (*a*) and (*b*)—galaxies showing good line-width, critical-density correlations—represent unweighted linear least-squares fits to data. Data in (*c*) appear uncorrelated.

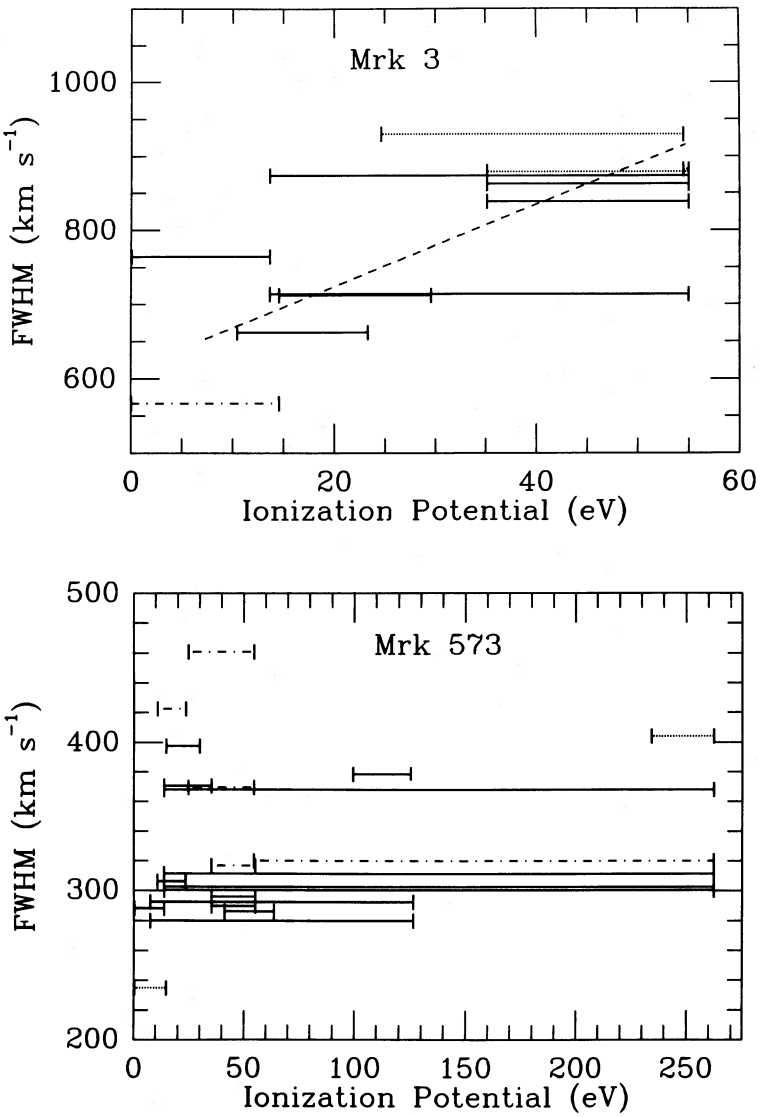

FIG. 2.—Correlations of emission-line widths at half-maximum (FWHM) with mean ionization potential (see text for definition) for (*a*) Mrk 3 and (*b*) Mrk 573. Horizontal lines connect lower and upper stages of ionization for ions indicated by vertical bars. Lines of H I, He I, and He II are included using an upper ionization potential equal to the maximum observed in the galaxy. Solid lines represent profiles of quality 1, dash-dot lines quality 2 profiles, and dotted lines quality 3 profiles. Diagonal dashed line in (*a*) represents unweighted linear least-squares fit to data. Data in (*b*) appear uncorrelated.

a) NGC 2110

This was originally an X-ray selected galaxy. It was called a Seyfert 2, but Shuder (1980) detected a weak, broad, Hα emission-line component. [N I] λ5199 and [S II] λλ4069, 4076 and λλ6716, 6731 are strong relative to Hα. He II emission is very weak, and there is no evidence for [Fe VII]. There is a hint of a blueward asymmetry at base of [O III] λλ4959, 5007 with our resolution. The [O I] λ6300 profile is among the broadest of the emission lines.

b) NGC 5506

This also was originally an X-ray selected galaxy. Like NGC 2110, this Seyfert 2 was noted to have a weak, broad, Hα emission-line component by Shuder (1980). The emission-line widths for NGC 5506 are all less than 400 km s^{-1}. There is certainly He II emission, but little if any [Fe VII]. [S II] λλ6716, 6731 are relatively strong. The [O III] λλ4959, 5007 profiles show a very slight blueward asymmetry near the continuum level. There is some evidence for [S III] λ6312.

c) NGC 7212

NGC 7212 has moderately broad line profiles, especially [S II] λ4069 which is probably contaminated by [Fe V] λ4071. Although [Fe VII] λ6087 is rather weak, He II is well represented. There is a slight trace of a redward asymmetry in [O III] λλ4959, 5007, but [O I] λλ6300, 6364 both show larger (and similar) redward asymmetries. Weak He I λ6678 is seen.

d) NGC 7319

There does not appear to be any [Fe VII], and only marginal He II λ4686 in NGC 7319. Both [N I] λ5199 and [O III] λ4363 are rather weak. The profiles generally show a very slight blueward asymmetry.

e) Mrk 1

Mrk 1 has moderately broad emission-line profiles. [Ne III] λλ3869, 3967 are relatively strong, and [S II] λλ4069, 4076, although broad, are probably affected by [Fe V] λ4071. He II, [N I] λ5199, [Fe VII] λ6087 are weak. It is interesting to note that [O I] λλ6300, 6364 have a substantially blueward asymmetry, while most of the other profiles display only a slight blueward asymmetry.

f) Mrk 3

Of our entire Seyfert 2 sample, Mrk 3 has the broadest forbidden emission-line profiles. All of them show a substantial blueward asymmetry. [N II] λλ6548, 6583 are strong relative to Hα. There undoubtedly is [Fe VII] λ6087, but, because it is so broad, it is very difficult to measure.

g) Mrk 78

The emission-line profiles are all double-peaked, the result of emission from the nucleus of Mrk 78 and a secondary "cloud" $\sim 2''$ from the nucleus (Adams 1973). The nuclear emission-line profiles were deblended from the observed profiles, and these FWHMs are reported in Table 4. As a result, our FWHMs are substantially less than those listed in either Heckman *et al.* (1981) or Feldman *et al.* (1982). For a discussion of the morphology and emission-line spectrum see De Robertis (1985).

h) Mrk 348

Although He II emission is weak, its width is measurable. However, [Fe VII] λ6087 is too weak to permit a width determination. The [O I] λ6300 profile appears to consist of a rather narrow profile situated on a relatively broad base. There may be some evidence for a broad but weak component in the Hα profile. There are small blueward asymmetries in all the profiles.

i) Mrk 516

This Seyfert 1.8 galaxy appears to have neither He II nor [Fe VII] emission. The scans are somewhat noisy since this object is relatively faint.

j) Mrk 573

Mrk 573 is a relatively high ionization Seyfert 2 with narrow emission-line profiles. There is strong He II λ4686, [Fe VII] λ6087, and [Fe X] λ6375. [S II] λλ4069, 4076 are present, but the profiles are not very broad. In general, the line profiles tend to be symmetric. [N I] λ5199 is weak, and the indicated width is rather uncertain. [O I] λ6300 is definitely broader than [S II] λλ6716, 6731.

k) Mrk 1018

The appearance of the continuum in the Seyfert 1.9 galaxy, Mrk 1018, suggests that there must be a rather large stellar contribution. The H I lines are weak (undoubtedly with underlying Balmer absorption), and no He II λ4686 or [Fe VII] λ6087 is evident. Although [O I] emission is present, it is very weak, and the FWHM estimates are rather uncertain. [N II] λ6583 is very strong relative to Hα. There is little if any [O III] λ4363.

l) Mrk 1058

The spectra of Mrk 1058 reveal the presence of a large, integrated stellar contribution to the continuum. The H I emission lines are weak, as are He II λ4686 and [O I] λ6300. The line profiles are rather narrow, with [O I] the broadest of the profiles measured. [N II] is relatively strong compared with Hα. [O III] λ4363 is weak.

m) Mrk 1066

Mrk 1066 has only weak He II λ4686 and no [Fe VII]. [O I] λ6300 is among the broadest lines, certainly broader than [S II] λλ6716, 6731, which themselves appear to have somewhat different line profiles.

n) Mrk 1073

Mrk 1073 has a high-ionization spectrum. There is definite He II λ4686 and [Fe VII] λ6087 (although the latter profile is rather narrow), and there an indication that [Fe X] is present from the appearance of the red wing of [O I] λ6364. [S II] λλ4069, 4076 are moderately broad. [O III] λ4363 is rather weak. [N I] λ5199 appears broad, but, because it is so weak, the profile could not be measured. The [O I] profiles are only slightly broader than the [S II] lines. In general, the line profiles appear highly symmetric.

o) Mrk 1157

The profiles in Mrk 1157 (NGC 591) appear symmetric. There is certainly noticeable stellar contamination in the continuum. Both He II and [Fe VII] emission are present. There is marginal evidence that [Fe X] λ6375 is present in the red wing of λ6364. The spectra show that [O I] λ6300 is broader than most lines of lower ionization, although all the profiles are rather narrow in this object. [N I] λ5199 is weak, although [N II] λλ6548, 6583 are relatively strong.

p) I Zw 92

I Zw 92 (Mrk 477) has a very high ionization emission-line spectrum. [Ne V] λ3426, He II λ4686, [Fe VII] λ6087, and [Fe X] λ6375 are immediately evident. The continuum appears to be almost completely nonstellar. All the profiles have a large blue asymmetry at a low intensity level (see De Robertis 1985). [N I] λ5199 is weak, although measurable. Hα appears strong relative to [N II] λ6583. There appears to be a broad base on the [O I] λ6300 profile at a low intensity level, almost as if it is a double-component profile.

High signal-to-noise ratio data taken in 1980 March and 1985 February show a distinct difference in the relative strengths of the [Fe VII] λ6087 and [Fe X] λ6375 profiles in the sense that in the more recent the lines are weaker. Osterbrock and Pogge (1985) have noted a similar effect for [Fe X] λ6375 in the narrow-line Seyfert 1 galaxy Mrk 766. Such a variation in I Zw 92, when taken in conjunction with the excellent correlation found between the line width and critical density for this object, would seem to suggest that the high-ionization, relatively dense narrow-line gas ($\sim 10^7$–10^9 cm^{-3}) is situated ~ 1 pc from the photoionizing continuum.

q) UM 16

UM 16 is a relatively faint Seyfert 2 with a faint but noticeable stellar continuum. The line profiles appear highly symmetric. There is strong [Fe VII] λλ5721, 6087 (although λ5721 seems to be contaminated either by stellar features or by another emission line). Broad [Fe X] λ6375 is definitely present, but the profile is too noisy to measure accurately. The [O I] λ6300 profile is very narrow. [S II] λλ6716, 6731 do not appear to have profiles as similar as in the other Seyfert 2

spectra. Such profile differences might arise because the lines have somewhat critical densities.

r) Akn 347

There are weak but noticeable stellar absorption features throughout the continuous spectrum of Akn 347 (= NGC 4074). There are definite He II λ4686, [Fe VII] λ6087, and [N I] λ5199 emission lines. The line profiles tend to be symmetric, although they are quite narrow. [N II] λ6583 is stronger than Hα.

IV. NARROW EMISSION-LINE GALAXIES

The narrow emission-line galaxies of Table 2 were observed, and their emission-line profiles were measured using identical techniques to those used for the Seyfert galaxies of Table 1, largely as a control sample. As expected, in three of the narrow emission-line galaxies—NGC 6951, Akn 160, and Haro 25—the FWHMs are significantly smaller than in the Seyfert 2s. Note that in two cases the FWHM formally came out less than zero, the result of observing a small, nearly stellar nucleus in excellent seeing, and reducing the observed profile with an instrumental profile derived from a comparison lamp, which illuminates the slit of the spectrograph as a diffuse source. The instrumental profile derived in this way is broader than the observed profile, if the true FWHM is sufficiently narrow.

Of the other galaxies, M81 is an incipient Seyfert galaxy (Peimbert and Torres-Peimbert 1981; Osterbrock and Shuder 1981), and Mrk 309 is ionized by a large number of Wolf-Rayet or Of stars (Osterbrock and Cohen 1982) which may drive a weak galactic wind as well as their own well-known stellar winds. Thus it is not surprising to see line widths of order 300–400 km s^{-1} in these two objects. NGC 7177, however, is an apparently normal SB galaxy, with only weak emission lines of the type encountered in every spiral galaxy nucleus (Keel 1983). FWHMs of order 400 km s^{-1}, comparable to those near the low end of the range encountered in Seyfert 2 galaxies, are not expected in this apparently otherwise inactive galaxy. (Note that the emission-line widths given in Table 2 are minimum values because no corrections were made for any underlying absorption stellar features.) In fact, however, there is very little published information on line widths in such galaxies, and we intend to pursue this point by further observations of other similar objects.

We have not attempted any correlation analysis of the line-width data for these narrow emission-line galaxies; the number of objects and range of widths in each galaxy are both too small.

V. ANALYSIS AND DISCUSSION

For some of the Seyfert 1s in Paper I there appeared to be a distinctly better correlation between the narrow-line widths and the critical densities than between the widths and ionization potentials required to "produce" the ions. Indeed, [O III] λ4363 was found to be broader in almost every case than [O III] λ5007, and, for some objects, [O I] λ6300 was distinctly broader than other low-ionization lines such as [S II] λλ6716, 6731. Similar conclusions have been reached by Pelat, Alloin, and Fosbury (1981) for NGC 3783; Atwood, Baldwin, and Carswell (1982) for NGC 3783 and Mrk 509; Cohen and Marcy (1983) for Mrk 704 and MCG 8-11-11; Filippenko and Halpern (1984) for NGC 7213; and Filippenko (1985) for LINERs (low-ionization nuclear emission-line regions). On the other hand, some of the Seyfert 1s from Paper I appeared to show a better correlation between line width and ionization potential, with [O I] λ6300 among the narrowest of emission lines.

For the Seyfert 2 galaxies of the present paper we first investigated possible first-order critical density or ionization correlations with line width. The critical density analysis was handled as in Paper I. However, for the ionization potential investigation, instead of testing for a correlation between the line width and the ionization potential to *produce* the emitting ion, we have taken as a relevant measure the mean of the ionization potentials of the lower and upper stages of ionization (i.e., cols. [3] and [4] in Table 3). Since the upper stages of ionization for H I and He II are effectively infinite, we adopted for them a "representative" ionization potential for the upper stage equal to the maximum ionization potential observed in the optical spectrum of the galaxy. Our motivation for adopting this technique was to provide a better measure of threshold ionizing-photon energies in the emission line gas than would be provided by either the lower or upper ionization potential alone.

The results of the analysis show unquestionably that the FWHM–critical density correlation provided a better linear fit in a larger percentage of galaxies than the ionization potential correlation. Including both the good and weak correlations, over one-half of the galaxies with more than five measured lines showed a critical density correlation in the sense that lines of higher critical density have broader FWHMs. (A good correlation is here defined by an absolute value of the linear correlation coefficient greater than or equal to 0.60, a weak correlation between 0.40 and 0.60, and no correlation if less than 0.40.) Two galaxies showed a weak anticorrelation. Only one third showed no good or weak correlation. Figures 1*a*–1*c* display the critical density–FWHM relationship in three representative systems: (*a*) NGC 2110 and (*b*) I Zw 92, with very good critical-density correlations, and (*c*) UM 16, with a poor correlation. The unweighted linear least-squares fit to the data for NGC 2110 and I Zw 92 are indicated by dashed lines. In the galaxies with measurable [O III] λ4363 and λ5007, more galaxies had λ4363 broader compared with λ5007 than had λ4363 the same width or narrower than λ5007. Similarly, in galaxies with measurable [S II] λλ4069, 4076 and λλ6716, 6731, the former profiles were invariably much broader than the latter. [O I] λ6300 was, in many cases, broader than [S II] λλ6716, 6731.

The ionization potential correlations were significantly poorer, with fully two-thirds of the Seyfert 2 galaxies displaying no correlation whatsoever. Figures 2*a*–2*b* depict one of the few good ionization potential correlations, in Mrk 3, and a typical uncorrelated system represented by Mrk 573. The lack of good correlations does not appear to depend on the method to define the mean ionization potential. The qualitative status of the correlations is not improved by ignoring the H I, He I, and He II lines, in an attempt to make the ionization potential treatment symmetric with the critical density case. It appears then that in the main, Seyfert 2s show a distinct tendency toward critical density correlations similar to some Seyfert 1s in Paper I.

A simple quantitative way to see the effects involved is to imagine that the ionized gas in the "narrow-line region" is in clouds, and that the mean density within the clouds depends on r, their distance from the photoionizing source, according to a power-law

$$N \propto r^{-n} .$$

The ionization parameter at the face of such a cloud, which determines the degree of ionization of the various elements, is then

$$\Gamma \propto \frac{L}{4\pi r^2 N} \propto r^{n-2},$$

where L is the ionizing photon luminosity.

Thus if $n = 2$, the ionization parameter, and hence the ionization itself at the front faces of all the clouds, is independent of distance (in the absence of dust). If each cloud is optically thick to most of the ionizing radiation, the ionization decreases with increasing optical depth, and all clouds have (to a first approximation) the same ionization and thermal structure, scaled according to their density. Hence, even though the velocity of the clouds depends on distance, the line profiles would not depend on ionization at all. On the other hand, the density variation would lead to collisional de-excitation in clouds close to the photoionizing source and thus to a dependence of line profile with critical density. This is observed in many objects, in the sense that lines with higher critical densities have larger FWHMs; in other words, the mean observed radial velocity is largest near the center and decreases outward (Pelat, Alloin, and Fosbury 1981; Atwood, Baldwin, and Carswell 1982; Filippenko and Halpern 1984; De Robertis and Osterbrock 1984).

If, however, $n > 2$, then the ionization parameter Γ would increase outward, and high stages of ionization like Ne^{+4} and Fe^{+6} would not exist in clouds close to the central source. If the velocity field were the same as in the first case, the FWHM would *decrease* with increasing ionization potential; this situation is not observed in any Seyfert galaxy, and we therefore conclude $n > 2$ does not occur in nature.

If $n < 2$, Γ would decrease outward, high stages of ionization would occur only in clouds close to the central source, and, for the same type of velocity field, the FWHM would increase with increasing ionization potential. This *is* observed in many objects, which again shows that the mean observed radial velocity decreases outward. In an extreme case, if $n = 0$, there would be no density dependence on distance, and hence *no* correlation of FWHM with critical density.

In most Seyfert galaxies there is some dependence of FWHM on ionization potential, and some on critical density; hence, the density dependence is probably fitted roughly by a power law with $0 < n < 2$. More Seyfert 1 galaxies have FWHM correlated with ionization potential, that is, in these simple terms, have n closer to 0, while more Seyfert 2 galaxies have FWHM correlated with critical density, that is, have n closer to 2. This density dependence will be related to physical conditions within the ambient medium in the narrow-line region if the clouds are in pressure equilibrium with this medium (e.g., Krolik and Vrtilek 1984). If the "confining medium" is in the form of an isothermal outflowing wind, then the radial dependence on pressure is

$$P \propto r^{-n},$$

that is, identical to the cloud density. Current wind models appear able to account for $n \leq 2$ (Krolik and Vrtilek 1984). As these authors state, the observations are still far from uniquely determining the kinematics; models assuming inflow, outflow, or random motions can all be made to fit the data.

The [O I] λ6300 profiles individually are interesting. In Table 4 there are obvious instances in which [O I] λ6300 is substantially broader than [S II] $\lambda\lambda$6716, 6731 (e.g., Mrk 1). Cases in which [S II] $\lambda\lambda$6716, 6731 are apparently broader than [O I] λ6300 are almost always at a level consistent with the measuring errors; i.e., they have equal widths. In the cases in which λ6300 is only slightly broader than $\lambda\lambda$6716, 6731 (e.g., I Zw 92), it appears that the [O I] profile may be composed of two components: a narrow "core" similar in appearance to λ6716, or λ6731, on top of a significantly broader base or broad component. If this observation is correct, then the natural interpretation according to the discussion in Paper I is in terms of [O I] emission from two distinct regions: the narrow component originates in optically thin clouds with a low-velocity dispersion at relatively large distances from the continuum source (which are also responsible for the [S II] emission), and the broad component near the [O I] critical density originates in optically thick clouds with a relatively higher velocity dispersion closer to the continuum source. The relative integrated emissivity from each of the regions then determines the final structure of the observed profile. The two-component nature of the [O I] profile might explain why critical density correlations are not always better than those involving ionization potential. In general, the ratio of relative strengths of the broad and narrow components is a function of the shape of the ionizing continuum, the geometry (distribution) of the emission-line gas, and the relative distances of the gas from the continuum source. One might expect cases in which [O I] λ6300 and [S II] λ4069 emission from the dense (i.e., broad) region dominates the less dense (narrow) region, and vice versa. In some instances, in which [O I] λ6300 is just broader than [S II] $\lambda\lambda$6716, 6731, the emission is distributed between the two regions. One could imagine using very high-resolution, high-quality [O I] and [S II] profiles to study the distribution of gas within the narrow-line region. A more quantitative discussion of the relationship between narrow emission-line profile widths and physical conditions in the narrow-line region is given in the Appendix.

For each galaxy we have measured the equivalent widths of the Hβ and λ5007 emission lines, the equivalent widths of Mg I *b* λ5176 and, where available, the Fe I E2 λ5270 absorption lines, and the monchromatic continuum luminosity at 5000 Å based on $q_0 = 0$, $H_0 = 75$ km s^{-1} Mpc^{-1}. All of these data are recorded in Table 1. As noted previously, because the data were taken with a small slit size, the luminosities are probably accurate to of the order of 10%. In order to calculate the fraction of the featureless continuum present at 5000 Å, f_{FC}, we compared the measured absorption-line equivalent widths with corresponding widths in "template" galaxies with spectral classes K0 III and K5 III kindly provided by W. Keel. (Note that although the equivalent widths of the *b* and E2 lines in these templates and the Seyfert galaxies were measured in a consistent fashion, they may not be accurate in an absolute sense.) Values for f_{FC} based on *b* and, where available, E2, were calculated from the absorption line widths measured in the K0 III and K5 III galaxies. If there was near agreement between $f_{FC}(b)$ and f_{FC}(E2), we adopted this as the most probable value for f_{FC}. If there was not good agreement, or if we had an estimate based only on *b*, then we used the f_{FC} derived from the K5 III comparison. There is a large uncertainty associated with f_{FC} calculated in this manner, but it is a reasonable first-order attempt to estimate the luminosity of the nonstellar continuum. (It is apparent that the underlying stellar component is not the same for all the galaxies. For example, both Mrk 78 and UM 16 have essentially zero E2 equivalent widths, which

are not consistent with stellar continua dominated by early K III stars.)

There was a weak but consistent first-order correlation between the equivalent width of Hβ and the FWHMs of the narrow lines Hβ, [O III] λ5007, [O I] λ6300, [N II] λ6583, and [S II] $\lambda\lambda$6716, 6731. (The correlation between the observed equivalent width of Hβ and line widths was always better than between the reduced equivalent width expressed in terms of the featureless continuum and line widths. This may mean that the featureless continuum is not important in these Seyfert 2s, or, more likely, it may mean that the f_{FC} estimates are substantially in error.) An interesting feature of all five correlations is the similarity of their velocity intercepts (i.e., the FWHMs corresponding to an equivalent width of 0 Å for Hβ): 320 $\pm$ 25 km s^{-1} (where we have quoted the formal error).

As for the physical implications of the correlation, it must be connected with the nature of the acceleration mechanism ultimately responsible for the emission-line widths in Seyfert galaxies. In a spherically symmetric picture, this velocity might be identified with the minimum velocity the emission-line gas clouds acquire from the acceleration mechanism. If the narrow-line gas is confined to a planar or cylindrical volume, then this lower limit might correspond to the "turbulent" velocity dispersion perpendicular to the principal plane. Osterbrock (1978) and Tohline and Osterbrock (1982) have remarked that disklike emission-line regions with a significant turbulent velocity component, or such regions which are not necessarily aligned with the underlying stellar galactic disk, need not show a correlation between inclination and line width.

This could explain why some high-ionization Seyfert galaxies like Mrk 573 and Mrk 1388 (Osterbrock 1985) have profiles as narrow as, or narrower than, non-Seyfert galaxies like NGC 7177. Further, the "uniqueness" of the intercept would seem to indicate that there is a minimum FWHM for emission lines in Seyfert phenomenon, 320 km s^{-1}, very similar to the often quoted value noted in § I. Phillips, Charles, and Baldwin (1983) and Whittle (1985*a*, *b*) have found some lower luminosity Seyfert galaxies to have [O III] λ5007 FWHMs significantly smaller than 300 km s^{-1}, like Mrk 1058 in our sample. De Robertis and Osterbrock (1986) have found in NGC 1320 a very high ionization (although feeble) Seyfert 2 in which there are a number of line widths less than 300 km s^{-1}. It is not clear what fraction of Seyfert 2s share these characteristics, but currently they make up only a small fraction of the number of known objects of this class.

There are no significant correlations between any of the other measured parameters, expressed either in terms of the featureless or of the apparent continuum and the velocity width. (Neither did there appear to be any correlation between the inclination of the disk of the Seyfert galaxy and emission-line widths. This is consistent with previous studies of the narrow-line region; e.g., Heckman *et al.* 1981; Miley and Heckman 1982; Heckman, Miley and Green 1984.)

VI. COMPARISON OF SEYFERT 1 AND 2 GALAXIES

Finally, we may ask the question whether narrow-line profiles in Seyfert 2s and Seyfert 1s are similar, i.e., are taken from the same underlying distribution. Heckman *et al.* (1981) have found the [O III] λ5007 FWHMs are different, while Whittle (1985*b*), arguing that they have omitted low-luminosity Seyfert 2s, has found the distributions the same. A complete sample of Seyfert 1s and 2s measured in a homogeneous way might provide an unambiguous answer to this question. There is no way of determining even whether the Seyfert 1 galaxies in Paper I or the Seyfert 2 galaxies of this paper constitute representative samples from their own underlying distributions, since they were discovered with inhomogeneous techniques and then selected by us for their high ionization. We shall, nevertheless, make the tentative assumption that the samples are representative. Another important point to note is that the widths of the emission lines in these two papers were measured by different methods. There is reason to believe that there is a small systematic difference between the deconvolution measurements of the Seyfert 1 galaxies of Paper I and the "quadrature" measurements of the Seyfert 2 galaxies of this paper. Osterbrock and Pogge (1985) have determined the line widths using this quadrature method for two galaxies also measured in Paper I by deconvolution techniques. According to their results, there appears to be a systematic difference in the methods, with the deconvolution quadrature yielding widths smaller by $\sim$40 km s^{-1} (if measured on a high-dispersion scan, with a resolution of $\sim$5 Å as in the present paper) than the presumably more nearly correct deconvolution method.

Because we are not aware of the *a priori* underlying distributions, a nonparametric statistical test is indicated. A widely used test in this situation is the Wilcoxon rank sum (RS) test. In it (Lehmann 1975), the FWHMs from each sample are assigned a rank relative to the combined sample: i.e., the largest width is assigned a rank of 1, second largest rank 2, and so on, without regard to sample origin. In the event that the data have been drawn at random from the same population, it can be shown that the sum of the ranks for a particular sample should be normally distributed with a well-defined mean and variance. By calculating the appropriate test statistic, one can then make a statement regarding the probability of that result on the assumption that the samples were chosen at random from the same underlying distribution.

The data to be tested in this case are the FWHMs for six narrow lines representing a wide range of ionization—[O II] λ3727, [O III] $\lambda\lambda$4363, 5007, [Fe VII] λ6087, [O I] λ6300, and either [S II] λ6716 or λ6731 (where available)—from each galaxy from the Seyfert 1 and Seyfert 2 samples. The RS test was performed for each of the six lines. Since the line widths for each sample were derived using different techniques, we expect a systematic difference between the velocity scales (see above). In an attempt to parametrize any possible FWHM difference and to obtain an estimate of the degree of sensitivity of the probability estimates, a "velocity offset" parameter was introduced: a fixed but arbitrary constant. In our analysis, this constant was *added* to the FWHMs of the Seyfert 1 sample, and these "artificial" FWHMs were then compared via the RS test with the Seyfert 2 FWHMs as measured. The results of the tests are summarized in Table 5. Column (1) lists the wavelengths for the lines that were tested, while columns (2) and (3) give the total number of the Seyfert 1 and 2 galaxies with a measured FWHM in the line.

Column (4) gives v_{min}, the lower velocity offset defined such that the probability of randomly choosing the samples is only 0.10, given the initial hypothesis (i.e., assuming they are from the same distribution). Column (5) gives v_0, the velocity offset such that the probability is 0.50 (the maximum probability), while column (6) provides v_{max}, the upper velocity offset such that the probability of randomly choosing the samples is only 0.10, given the initial hypothesis. (Thus v_0 may also be

TABLE 5

STATISTICAL COMPARISON OF LINE PROFILES

Wavelength (Å) (1)	Number of Seyfert 1 Galaxies (2)	Number of Seyfert 2 Galaxies (3)	v_{min} (km s^{-1}) (4)	v_0 (km s^{-1}) (5)	v_{max} (km s^{-1}) (6)
3727.....	12	8	−90	+30	+80
4363.....	11	12	−260	−150	−60
5007.....	12	14	−40	+60	+120
6087.....	12	7	−300	−150	+60
6300.....	11	14	−75	+25	+90
6716.....	12	14	+10	+60	+130

described as the velocity offset required to make the means of each sample equal.) Velocity offsets less than v_{min} or greater than v_{max} lead to probabilities *less than* 0.10, suggesting that is it unlikely that the samples could have been chosen at random from the same underlying distribution.

Table 5 indicates two different trends: the results from [O II] λ3727, [O III] λ5007, [O I] λ6300, and to some extent [S II] λ6716 suggest that there is a high probability that the FWHMs of both samples do come from the same population for velocity offsets of ± a few tens of km s^{-1}. The probabilities for these four lines are maximum for a mean velocity offset of +45 km s^{-1}; that is, an offset of +45 km s^{-1} gives the highest probability that the samples come from the same distribution.

Thus the mean FWHM of these four narrow emission lines in the Seyfert 1s, measured by the deconvolution technique of Paper I, is 45 km s^{-1} smaller than the mean FWHM of the same four lines in the Seyfert 2s, measured by the quadrature technique of the present paper. Taking into account the 40 km s^{-1} difference between the results of the two techniques mentioned above, the mean FWHM of these lines in the Seyfert 1s is smaller than mean FWHM in the Seyfert 2s by ∼85 km s^{-1}. The mean of the FWHMs, reduced to a common deconvolution method, is 395 km s^{-1} for the Seyfert 1s and 490 km s^{-1} for the Seyfert 2s.

Such a difference between the mean FWHM of [O III] λ5007 in Seyfert 1 and 2 galaxies was reported by Heckman and Balick (1979), Heckman *et al.* (1981), and Feldman *et al.* (1982). Heckman *et al.* (1981) found a mean FWHM of 380 km s^{-1} and 620 km s^{-1} for λ5007 for Seyfert 1 and 2 galaxies, respectively. Feldman *et al.* (1982), for a larger sample but with some overlap with Heckman *et al.*, found 375 km s^{-1} and 510 km s^{-1}, respectively, also for [O III] λ5007. Our results confirm this difference, and extend it to the lower ionization lines [O II] λ3727, [S II] λ6716, and [O I] λ6300. Although there is large difference between the mean FWHMs, the formal dispersions about the means given in Heckman *et al.* (1981) and Feldman *et al.* (1982) for both Seyfert 1s and 2s are also large, ∼225 km s^{-1}. For the Seyfert 1s of Paper I and the Seyfert 2s of this paper, the dispersion is ∼160 km s^{-1}. Adopting the null hypothesis that the Seyfert 1 and 2 FWHMs of both Heckman *et al.* (1981) and Feldman *et al.* (1982) come from the same underlying distribution, and applying the RS test to each of these data indicate that the probability of randomly selecting the observed FWHMs from the same underlying distribution is only of the order of 1%. Although the same probability estimate for our data is somewhat higher (see Table 5), our results are qualitatively similar. It is interesting to note that the mean FWHM for the narrow emission lines of only high-ionization Seyfert 1s from Paper I is almost identical with the mean FWHM from the more varied samples of Heckman *et al.* (1981) and Feldman *et al.* (1982) containing many low-ionization Seyfert 1s, and the mean FWHM for the lower ionization lines in the relatively high-ionization Seyfert 2s is not significantly different from the Seyfert 2s in these same studies.

The second trend shown in Table 5 is that the probabilities that the FWHMs of the [O III] λ4363 and [Fe VII] λ6087 are drawn from the same underlying distribution are small. With the correction +40 km s^{-1} to the quadrature results mentioned above, the mean FWHMs of [O III] λ4363 and [Fe VII] λ6087 both are 110 km s^{-1} larger than in the Seyfert 2s. These differences are in the opposite sense from the [O I] λ6300, [S II] λ6716, [O II] λ3727, and [O III] λ5007 lines. Both [O III] λ4363 and [Fe VII] λ6087 are lines combining high ionization potential and high critical density, and they probably originate in a region between the classical broad- and narrow-line regions. The internal velocities in an average Seyfert 1, in comparison with an average Seyfert 2, are higher in this region.

It is not clear what causes these differences in FWHM between Seyfert 1s and 2s. Heckman *et al.* (1981) and Ulvestad and Wilson (1984) have suggested that the power associated with the steep-spectrum, kiloparsec-sized radio source may play a role here. Since Seyfert 2s are, on average, stronger radio sources, perhaps the nonthermal pressure associated with these sources provides an additional acceleration mechanism or confining pressure for the low-ionization, low critical-density clouds, thereby leading to border emission lines. Clouds of higher density and velocity dispersion closer to the continuum source must not be similarly affected in Seyfert 2s and, in fact, may be retarded by the additional pressure. It is also possible, however, that the differences between Seyfert 1 and 2 galaxies may result from significant differences in the geometry or distribution of the gas within the emission-line regions.

The result that there are statistically significant differences between the line profiles in Seyfert 1 and 2 galaxies may provide an important time scale constraint for evolution between Seyfert types. On the basis of a statistical difference between the radio structures of Seyfert 1s and 2s, de Bruyn and Wilson (1978) have argued that evolution between types would require time scales $\geq 10^5$ yr—the time required to appreciably change the radio structure. In the same way, the time scale for changes to the narrow-line profile widths must be at least 10^5 yr (the velocity of the narrow-line gas divided by the size of the narrow-line region). We emphasize that this argument holds only in a statistical sense and does not preclude the possibility that individual objects can apparently "change types" on much shorter time scales. A similar argument can be made from these observations that Seyfert 2s are not highly reddened Seyfert 1s.

VII. SUMMARY

Emission-line profiles have been measured in 18 Seyfert 2 galaxies, most having a high-ionization spectrum. Correlations were found between emission-line width and critical density for approximately two-thirds of the galaxies in the sample with more than five measured emission lines. In contrast, only a couple of galaxies showed a correlation between line width and ionization potential. As in the case of high-ionization Seyfert 1 galaxies (Paper I), a large fraction of Seyfert 2s have broader [O III] λ4363 compared with [O III] λ5007, and broader [O I] λ6300 compared with [S II] λ6716. It was argued that this follows from a mode of the narrow-line region in which most of the emission originates in optically thick emission-line clouds such that higher density clouds have a larger velocity dispersion. Galaxies with narrow [O I] λ6300 must have substantial quantities of optically thin emission-line gas with a relatively low velocity dispersion.

Equivalent widths for Hβ, [O III] λ5007, the monochromatic continuum luminosity at 5000 Å, and the fraction of the featureless continuum at 5000 Å (estimated using the equivalent widths of the Mg I *b* and Fe I E2 absorption features) were measured for each galaxy. No significant correlations were found between the emission-line widths and other measured galaxy parameters expressed in terms of either the observed or featureless continuum, except a correlation between the Hβ emission-line equivalent width and the line widths for *all* emission lines: viz., as the Hβ emission-line equivalent width tends to zero, all the narrow-line widths converge to 320 ± 25 km s^{-1}. This result (which was in good agreement with an earlier Seyfert 2 selection criterion of Shuder and Osterbrock 1981) might be interpreted as the minimum velocity imparted to the emission-line clouds and filaments by the acceleration mechanism in a spherically symmetric geometry, or, for flattened emission-line regions, the velocity dispersion perpendicular to the plane.

The nonparametric Wilcoxon rank sum test was used to test the hypothesis that the Seyfert 2 line profile widths and the corresponding Seyfert 1 narrow-line profile widths from Paper I were selected from the same underlying distribution. It was found that the probability is highest if the observed distribution of low-ionization emission-line widths in Seyfert 2 galaxies has a somewhat higher mean than for Seyfert 1s, although the range within each type is large. For lines of high ionization *and* critical density, [O III] λ4363 and [Fe VII] λ6087, the Seyfert 1 galaxies on average have larger FWHMs. The significant profile differences between Seyfert 1s and 2s argue in a statistical sense against evolution between types on short time scales, and that Seyfert 2s are not highly reddened Seyfert 1s.

Seyfert 2s necessarily have a high-ionization spectrum and broad lines. In a comparison sample of a few "narrow emission-line" galaxies taken with similar parameters, FWHMs in excess of 320 km s^{-1} were also found (e.g., NGC 7177). Thus, line width is a necessary but not sufficient condition for the Seyfert phenomenon. It was noted that the distribution of nuclear emission-line widths in non-Seyferts is not well known.

Finally, [Fe X] λ6375 and [Fe VII] λ6087 were found to vary substantially in I Zw 92 on time scales of a few years, indicating that the high-ionization narrow-line region may have dimensions of a couple of parsecs.

We are indebted to W. G. Mathews, J. S. Miller, and O. Dahari for many stimulating and profitable discussions on the subjects included in this paper. We are also grateful to the National Science Foundation for partial support of this research under grant AST 83-11585.

APPENDIX

EFFECTIVE ELECTRON DENSITIES

As stated in the body of the paper, [S II] $\lambda\lambda$6716, 6731 often are significantly narrower than other forbidden lines in Seyfert 1 and 2 galaxies. Also [O III] λ4363 is often significantly wider than $\lambda\lambda$4959, 5007. These differences can, in many situations, be attributed to the effects of collisional de-excitation, suppressing a line relative to other lines in the regions of higher density. Such observational evidence forms the basis for the statement that there is a positive correlation between radial velocity dispersion and electron density. For any specific model, calculations taking account of collisional excitation and de-excitation, as well as downward radiative transitions, give the populations of the individual ionic energy levels, and thus the emission rates, as functions of electron density and temperature. However, to see the main physical effects, it is instructive to consider the simple example of a two-level ion, in an assumed isothermal spherical narrow-line region with a power-law electron-density distribution.

Consider a two-level ion, with ground level 1 and excited level 2, emitting a line with energy $h\nu = E_2$ and transition probability A_{21}. The collisional excitation rate per unit volume may be written

$$N_e N_i q_{12} = N_e N_i \frac{8.63 \times 10^{-6}}{T^{1/2}} \frac{\langle \Omega(1, 2) \rangle}{\omega_1} e^{-E_2/kT}$$

in terms of the collisional strength $\Omega(1, 2)$, the statistical weight of the ground level ω_1, the temperature T, and the electron and ion densities N_e, N_i. The emission coefficient per unit volume in the line may then be written

$$4\pi j = N_e N_i q_{12} h\nu \left(1 + \frac{N_e q_{21}}{A_{21}}\right)^{-1} = N_e N_i q_{12} h\nu \left(1 + \frac{N_e}{N_c}\right)^{-1},$$

where

$$q_{21} = \frac{\omega_1}{\omega_2} q_{12} e^{E_2/kT},$$

and

$$N_c = \frac{A_{21}}{q_{21}}$$

is the critical density for collisional de-excitation of the excited level (see, e.g., Osterbrock 1974).

First consider a situation in which the temperature and degree of ionization are both constant, so q_{21}, q_{21}, and N_c are constants, and $N_i = fN_e$, where f is a constant. Then

$$j = cfN_e{}^2\left(1 + \frac{N_e}{N_c}\right)^{-1} = \frac{ax^2}{1+x},$$

where c and $a = cfN_c{}^2$ are constants, and $x = N_e/N_c$.

Suppose $N_e = N_e(r)$; i.e., the density is a function only of distance from the center r in a spherically symmetric model. Also suppose the "dilution factor" is constant. Then L, the luminosity of the model in the line, can be written

$$L = \int j dV = \int_0^\infty \frac{ax^2}{1+x}\, dV = 4\pi a \int_0^\infty \frac{x^2}{1+x}\, r^2 dr .$$

Suppose the density variation can be represented by a power law $N_e \propto r^{-n}$, with $n \geq 0$, so the density decreases outward, or

$$x = Br^{-n},$$

with B a constant. Then

$$L = \frac{4\pi a}{n} B^{3/n} \int_0^\infty \frac{x^{(1-3/n)}}{1+x}\, dx .$$

One special case is $n = 3$. For it,

$$L = \frac{4\pi aB}{3}\Big[\ln(1+x)\Big]_0^\infty .$$

This diverges as $x \to \infty$ ($r \to 0$); that is, in this case the maximum contribution comes from the regions of *highest* density, close to the center, in any model of this form with a cutoff at a finite r (finite N_e).

Another special case is $n = 3/2$. For it,

$$L = \frac{8\pi aB^2}{3}\left[\ln\left(\frac{1+x}{x}\right)\right]_0^\infty .$$

This diverges as $x \to 0$ ($r \to \infty$); the maximum contribution comes from the regions of *lowest* density, far from the center, in any model of this form.

An intermediate case is $n = 2$. For it,

$$L = 2\pi^2 aB^{3/2} .$$

Thus comparing the ratios of two lines of the same ion, I and II, such as [O III] λ5007/[O III] λ4363, or [S II] λ6716/[S II] λ6731, in this simple approximation gives

$$\frac{L_{\rm I}}{L_{\rm II}} = \frac{a_{\rm I}}{a_{\rm II}} \frac{B_{\rm I}{}^{3/2}}{B_{\rm II}{}^{3/2}} = \frac{c_{\rm I}}{c_{\rm II}} \sqrt{\frac{N_{c\rm II}}{N_{c\rm II}}} .$$

Note the high-density limit of the ratio of strengths of these two lines is

$$\frac{j_i}{j_{\rm II}} \to \frac{c_{\rm I}}{c_{\rm II}} \frac{N_{c\rm I}}{N_{c\rm II}} \quad \text{as} \quad N_e \to \infty .$$

On the other hand, the low-density limit is

$$\frac{j_{\rm I}}{j_{\rm II}} \to \frac{c_{\rm I}}{c_{\rm II}} \quad \text{as} \quad N_e \to 0 .$$

Thus for this power-law model with $n = 2$, the ratio $L_{\rm I}/L_{\rm II}$ is the *geometric mean* of the high- and low-density limits of the ratio. Another way to put it is that $L_{\rm I}/L_{\rm II}$ is the ratio for an effective density:

$$N_e = \sqrt{N_{c\rm I}\, N_{c\rm II}} ,$$

that is, the *geometric mean* of the critical densities for the upper levels of the two lines.

Thus, to summarize, for an assumed spherical power-law form for the electron density distribution $N_e \propto r^{-n}$, with constant ionization and temperature,

1) If $n \leq 3/2$, the line ratio tends toward the limiting ratio for $N_e \to 0$, that is, for $r \to \infty$;

2) If $n = 2$, the ratio becomes that at the electron density which is the geometric mean of the critical densities of the two upper levels involved;

3) If $n \geq 3$, the ratio tends toward the limiting ratio for $N_e \rightarrow \infty$, that is, for $r \rightarrow 0$.

Now suppose the ionic abundance $f \neq$ constant, but instead $f = f(r)$. Then the simple power-law behavior no longer holds for N_i, and the behavior of the ratio depends on ionization, but if both N_{cI} and N_{cII} are within the range of r in which the variation of f is not large, then the above behavior persists approximately. Otherwise the ratio depends on the form of $f(r)$, but a power law with $N \leq 3/2$ always pushes the ratio toward $N_e \rightarrow 0$, $n \leq 3$ pushes the ratio toward $N_e \rightarrow \infty$, and intermediate indices $3/2 < n < 3$, that is $n \approx 2$, push toward the mean critical density.

Thus, as is obvious physically, the region with density near the critical density of any level is most effective in the emission of the line (or lines) arising in that level. The [S II] $\lambda 6716/\lambda 6731$ ratios in nearly all Seyfert 1 and Seyfert 2 galaxies are not near the high-density limit 0.35, nor the low-density limit 1.47, but are nearly always closer to an intermediate value of ~ 1, which corresponds to the mean critical density of the two ^2D levels, $[N_e(^2D_{5/2})N_e(^2D_{3/2})]^{1/2} \approx 2 \times 10^3$ cm^{-3}. Thus the line profiles of these lines come chiefly from regions around this density. On the other hand, [O III] $\lambda\lambda 4959$, 5007 represent a mean velocity dispersion from regions around $N_e \approx 7 \times 10^5$ cm^{-3}, but [O III] $\lambda 4363$ is more affected by the velocity field around $N_e \approx 3 \times 10^7$ cm^{-3} so long as there is gas at this and higher densities in the Seyfert galaxy.

REFERENCES

Adams, T. F. 1973, *Ap. J.*, **179**, 417.
Atwood, B., Baldwin, J. A., and Darswell, R. F. 1982, *Ap. J.*, **257**, 559.
Baldwin, J. A., Phillips, M. M., and Terlevich, R. 1981, *Pub. A.S.P.*, **93**, 5.
Cohen, R. D. 1983, *Ap. J.*, **273**, 489.
Cohen, R. D., and Marcy, G. W. 1983, *Bull. AAS*, **15**, 654.
de Bruyn, A. G., and Wilson, A. S. 1978, *Astr. Ap.*, **64**, 433.
De Robertis, M. M. 1985, in preparation.
De Robertis, M. M., and Osterbrock, D. E. 1984, *Ap. J.*, **286**, 171.
———. 1986, *Ap. J.*, **301**, 98
Elvis, M., and Lawrence, A. 1985, preprint.
Feldman, F. R., Weedman, D. W., Balzano, V. A., and Ramsey, L. W. 1982, *Ap. J.*, **256**, 427.
Ferland, G. J., and Osterbrock, D. E. 1985, *Ap. J.*, **289**, 105.
Ferland, G. J., and Shields, G. A. 1985, in *Astrophysics of Active Galaxies and Quasi-Stellar Objects*, ed. J. S. Miller (Mill Valley: University Science Books), p. 1.
Filippenko, A. V. 1985, *Ap. J.*, **289**, 475.
Filippenko, A. V., and Halpern, J. P. 1984, *Ap. J.*, **285**, 458.
Heckman, T. M., and Balick, B. 1979, *Astr. Ap.*, **79**, 350.
Heckman, T. M., Miley, G. K., and Green, R. F. 1984, *Ap. J.*, **281**, 525.
Heckman, T. M., Miley, G. K., van Breugel, W. J. M., and Butcher, H. R. 1981, *Ap. J.*, **247**, 403.
Keel, W. C. 1983, *Ap. J.*, **269**, 466.
Koski, A. T. 1978, *Ap. J.*, **223**, 56.
Krolik, J. H., and Vrtilek, J. M. 1984, *Ap. J.*, **279**, 521.
Lehmann, E. L. 1975, *Nonparametrics: Statistical Methods Based on Ranks* (San Francisco: Holden-Day).
Malkan, M. A. 1983, *Ap. J.*, **268**, 582.
Miley, G. K., and Heckman, T. M. 1982, *Astr. Ap.*, **106**, 163.
Miller, J. S., and Antonucci, R. J. 1983, *Ap. J. (Letters)*, **271**, L7.
Miller, J. S., Robinson, L. B., and Schmidt, G. D. 1980, *Pub. A.S.P.*, **92**, 702.
Miller, J. S., Robinson, L. B., and Wampler, E. J. 1976, *Adv. Electronics Electron Phys.*, **40B**, 693.
Osterbrock, D. E. 1974, *Astrophysics of Gaseous Nebulae* (San Francisco: Freeman).
———. 1978, *Proc. Nat. Acad. Sci.*, **75**, 540.
———. 1985, *Pub. A.S.P.*, **97**, 587.
Osterbrock, D. E., and Cohen, R. D. 1982, *Ap. J.*, **261**, 64.
Osterbrock, D. E., and Pogge, R. W. 1985, *Ap. J.*, **297**, 166.
Osterbrock, D. E., and Shuder, J. M. 1982, *Ap. J. Suppl.*, **49**, 149.
Peimbert, M., and Torres-Peimbert, S. 1981, *Ap. J.*, **245**, 845.
Pelat, D., Alloin, D., and Fosbury, F. A. E. 1981, *M.N.R.A.S.*, **195**, 787.
Phillips, M. M., Charles, P. A., and Baldwin, J. A. 1983, *Ap. J.*, **266**, 485.
Pritchet, C. J., Mochnacki, S., and Yang, S. 1982, *Pub. A.S.P.*, **94**, 733.
Robinson, L. B., and Wampler, E. J. 1972, *Pub. A.S.P.*, **84**, 161.
Shuder, J. M. 1980, *Ap. J.*, **240**, 32.
Shuder, J. M., and Osterbrock, D. E. 1981, *Ap. J.*, **250**, 55.
Tohline, J., and Osterbrock, D. E. 1982, *Ap. J. (Letters)*, **252**, L49.
Ulvestad, J. S., and Wilson, A. S. 1984, *Ap. J.*, **278**, 544.
Whittle, M. 1985*a*, *M.N.R.A.S.*, **213**, 1.
———. 1985*b*, *M.N.R.A.S.*, **213**, 33.

M. M. De Robertis and D. E. Osterbrock: Lick Observatory, Board of Studies in Astronomy and Astrophysics, University of California, Santa Cruz, CA 95064